The skull evolution of oviraptorosaurian dinosaurs: the role of niche-partitioning in diversification

The skull evolution of oviraptorosaurian dinosaurs: the role of niche-partitioning in diversification

Waisum Ma[1], Stephen L. Brusatte[1], Junchang Lü[2†] & Manabu Sakamoto[3]

[1]School of GeoSciences, The University of Edinburgh, Edinburgh, United Kingdom

[2]Institute of Geology, Chinese Academy of Sciences, Beijing 100037

[3]University of Reading, Reading, United Kingdom

[†]Deceased

Running title: Skull evolution of oviraptorosaurs

Correspondence:

Waisum Ma, School of GeoSciences, The King's Buildings, University of Edinburgh, Edinburgh, United Kingdom

Telephone number: +44 07907995477

E-mail: w.ma.1@pgr.bham.ac.uk

Abstract

Oviraptorosaurs are bird-like theropod dinosaurs that thrived in the final pre-extinction ecosystems during the latest Cretaceous, and the beaked, toothless skulls of derived species are regarded as some of the most peculiar among dinosaurs. Their aberrant morphologies are hypothesized to have been caused by rapid evolution triggered by an ecological/biological driver, but little is known about how their skull shapes and functional abilities diversified. Here, we use quantitative techniques to study oviraptorosaur skull form and mandibular function. We demonstrate that the snout is particularly variable, that mandibular and upper/lower beak form are significantly correlated with phylogeny, and that there is a strong and significant correlation between mandibular function and mandible/lower beak shape, suggesting a form-function association. The form-function relationship and phylogenetic signals, along with a moderate allometric signal in lower beak form, indicate that similar mechanisms governed beak shape in oviraptorosaurs and extant birds. The two derived oviraptorosaur clades, oviraptorids and caenagnathids, are significantly separated in morphospace and functional space, indicating that they partitioned niches. Oviraptorids coexisting in the same ecosystem are also widely spread in morphological and functional space, suggesting that they finely partitioned feeding niches, whereas caenagnathids exhibit extreme disparity in beak size. The diversity of skull form and function was likely key to the diversification and evolutionary success of oviraptorosaurs in the latest Cretaceous.

Keywords: Theropoda, Dinosauria, beak, niche-partitioning, evolution, diversification

Introduction

Oviraptorosaurs are a group of coelurosaurian theropod dinosaurs that first appeared in the Early Cretaceous (Ji, Currie, Norell, & Ji, 1998; Xu, Cheng, Wang, & Chang, 2002) and later developed a huge diversity – more than 80% of the known oviraptorosaur taxa have been discovered in Late Cretaceous rocks, most of which belong to the derived subclades Oviraptoridae and Caenagnathidae. Basal oviraptorosaurs are small-bodied forms that are currently only known from Asia, whereas the derived subclades dispersed across Asia and North America and exhibited great variation in osteological features and body sizes. Oviraptorosaurs are iconic animals known from remarkable fossils, some of which are covered in feathers or preserved brooding their nests in the same style as modern birds, and were among the final major wave of dinosaur diversifications before the end-Cretaceous asteroid impact killed off the non-avian species.

Oviraptorosaurs exhibit skull forms that deviate strongly from other non-avian theropods: their skulls are relatively robust and tall, and show different levels of tooth reduction (Brusatte, Sakamoto, Montanari, Harcourt, & William, 2012; Foth & Rauhut, 2013; Osmolska, Currie, & Barsbold, 2004; Xu et al., 2002). Derived oviraptorosaurs – caenagnathids and oviraptorids – possess an edentulous beak and sometimes a tall cranial crest, which is pneumatized and elaborated into a variety of shapes and sizes (Lü et al., 2017; Ma et al., 2017; Osmolska et al., 2004). The unusual skulls of oviraptorosaurs probably enabled distinctive diets compared to most theropods, although feeding habits are controversial. Direct evidence of herbivory is known in some basal oviraptorosaurs (Ji et al., 1998; Ji, Lü, Wei, & Wang, 2012; Xu et al., 2002), and diets such as herbivory, carnivory, omnivory and durophagy have been proposed for advanced oviraptorosaurs based on their osteological features (Funston & Currie, 2014; Funston, Currie, & Burns, 2015; Lee et al., 2019; Osmolska et al., 2004; Zanno & Makovicky, 2011).

Previous work has detected an exceptionally high rate of cranial evolution in derived oviraptorosaurs relative to other non-avian theropods, which was hypothesized to be caused by an ecological or biological driver (Diniz-Filho et al., 2015). However, the possible drivers of this rapid rate shift have never been investigated in detail. Previous studies have also demonstrated that the cranial form (shape) of theropods is strongly correlated with phylogeny, whereas the relationship between cranial form and function is more controversial (Brusatte et al., 2012; Foth & Rauhut, 2013). Given the aberrant nature of oviraptorosaurian skulls (Brusatte et al., 2012; Foth & Rauhut, 2013; Osmolska et al., 2004), it is unclear whether their skull forms experienced similar evolutionary constraints (i.e. phylogeny) as in theropods generally. These questions remain because the mechanisms underpinning the evolution and diversification of oviraptorosaur skulls are still poorly known and lack quantitative assessment. Answering these questions will clarify the evolutionary history of these unusual theropods. Furthermore, as oviraptorosaurs are some of the few non-avian dinosaurs that developed a completely toothless skull as in extant birds (Wang et al., 2017), understanding their history may give important insight into whether similar patterns and processes operated in independent clades of toothless dinosaurs.

In this study, we use quantitative methods to assess patterns of skull form and mandibular functional variation in oviraptorosaurs. We compare the morphospace occupation between major clades/grades to assess whether niche-partitioning likely occurred among oviraptorosaurs. We then use a series of statistical tests to evaluate the phylogenetic signals in the form datasets, as well as the correlations between form and function. The influence of body size, which is potentially correlated with skull form variation, is also assessed. This study illuminates the evolution of some of the most aberrant dinosaur skulls and examines how feeding-related niche-partitioning might have facilitated the diversification of oviraptorosaurs during the Late Cretaceous, during the last

few tens of millions of years before the dinosaur extinction, particularly in Asia where many taxa often lived contemporaneously.

Materials and methods

Specimens

We included every well-preserved, published, subadult or adult oviraptorosaur skull specimen in our analysis (see the electronic supplementary material, Table S1). Juvenile specimens were excluded, to minimize the possibility that observed morphological and functional variations are ontogenetic in nature, as at least some oviraptorosaurs exhibit high variation in mandible morphology across ontogeny (Wang, Zhang, & Yang, 2018). Thus, species known only from perinatal specimens (e.g. *Yulong mini* (Lü, Currie, et al., 2013) & *Beibeilong sinensis* (Pu et al., 2017)) were excluded from the analysis.

2D geometric morphometric analysis

We conducted geometric morphometric analysis to quantify the pattern of skull shape variation among oviraptorosaurs. The skull form of oviraptorosaurs was captured by plotting homologous landmarks on the lateral profile of the skulls in two-dimensional view (Figures 1, S1 & S2; Tables S2-5). We did not place landmarks on the cranial crest region, as their morphologies are extremely variable among oviraptorosaurs (Osmolska et al., 2004) and it has been suggested that the prominent crest of *Corythoraptor jacobsi* likely served sociosexual functions (rather than biomechanical functions) (Lü et al., 2017); this is also likely the case for other oviraptorosaurs

with elaborate crests. Excluding the crest region prevents the plausibly more feeding-related functional signals from being masked by the extreme crest variations. To detect any discrepancy in variation patterns of different parts of the skull, we divided the skull of oviraptorosaurs into four parts for separate geometric morphometric analyses: 1) cranium, 2) mandible, 3) upper beak and 4) lower beak (Figure 1; Table S6). By having four individual datasets, correlations with phylogeny and mandibular function could also be investigated separately. For each dataset, the images were compiled in the software tpsUtil (version 1.74) and imported into tpsDig (version 3.20) for landmark digitization (Rohlf, 2017). Procrustes fit was produced to standardise the landmark data using the software MorphoJ (Klingenberg, 2011). A covariate matrix was generated and lastly subjected to principal component analysis (PCA). The output principal component (PC, hereafter) scores serve as a proxy for the variation in form of oviraptorosaur skulls, which were used for further analyses to explore the correlations between form, function and phylogeny. See the electronic supplementary material section 2 for detailed methods.

Functional analysis

We quantified the functional variation among oviraptorosaur mandibles using functional characters. We developed 13 functional characters to capture different aspects of the mandibular functions of oviraptorosaurs (Note S1). All chosen characters have been demonstrated to provide feeding-related functional implications in extant animals and/or inferred in extinct animals (Note S1). We assessed these characters on 15 well-preserved mandibular specimens (Table S6). We then subjected the standardised measurements to principal coordinate analysis (PCoA), using the software PAST 3.18 (Hammer, Harper, & Ryan, 2001) (Note S2). Additional analysis was

conducted to estimate the contribution of each functional character to the first two principal coordinate (PCO hereafter) axes (Note S3).

Morphological and functional niche partitioning assessment

We conducted non-parametric multivariate analysis of variance (NPMANOVA, also known as perMANOVA) to assess the degree of overlap in both the morphological and functional morphospaces between major oviraptorosaur clades/grades (i.e. basal oviraptorosaurs, caenagnathids and oviraptorids) (Table S1). This allows us to test for possible niche-partitioning. Two analyses were conducted for each pair: PC1-2/PCO1-2 and all significant PC/PCO, which are defined as the first n PC/PCO explaining more than 90% of the total variance in the PCA/PCoA. We conducted the NPMANOVA tests in PAST 3.18 (Hammer et al., 2001). A significant result of the NPMANOVA test signifies that the two groups are significantly separated in morphological/functional space, which is consistent with niche partitioning. We adopt a 95% confidence level as a standard for all the statistical tests in this study. The null hypothesis is rejected if the p-value is <0.05. All of the p-values were corrected for multiple comparisons in R using the Benjamini-Hochberg procedure.

Evolutionary models of skull form

We used multiple phylogenetic comparative methods to evaluate the strength and significance of the correlations between phylogeny and different parts of the skull. For all the following analyses, we used the cladogram in Lü *et al.* (Lü et al., 2017) to represent phylogeny (Figure S3), which we time-calibrated (Note S4).

We used Blomberg's K statistic to evaluate the strength of the phylogenetic signal in the oviraptorosaur skull form datasets. Blomberg's K statistic is a measure of phylogenetic signal in a trait dataset (Blomberg, Garland, & Ives, 2003). A K larger than one indicates a strong phylogenetic signal, whereas K smaller than one implies otherwise (Blomberg et al., 2003). Each PC was subjected to the test individually, which allows us to identify PCs that exhibit a particularly strong/weak phylogenetic signal. A corresponding p-value was also calculated for each analysis. We performed these analyses using the 'picante' package in R (Kembel et al., 2010). Additional permutation tests were conducted to assess the correlation between overall skull form (represented by PC scores from PCA) and phylogeny (Note S5) in MorphoJ (Klingenberg, 2011), which follows the permutational procedures suggested by (Laurin, 2004).

Allometry

Skull shape of animals is often correlated with size, and thus some of the PC axes generated from the skull form datasets may be allometric in nature. This phenomenon has been observed in some extant birds, for example (Bright, Marugán-Lobón, Cobb, & Rayfield, 2016; Tokita, Yano, James, & Abzhanov, 2017). Thus, we are interested in knowing whether similar patterns also characterise oviraptorosaurs. We used centroid size as a measure of specimen size, which in turn acts as a proxy for body size, as utilised in a previous study on theropod skulls (Brusatte et al., 2012). However, as some of the form datasets may have strong phylogenetic signals, we employed the phylogenetic eigenvector regression (PVR) technique to extract the S-component (i.e. the model residuals, which is the phylogenetically-independent component) of these variables for further correlation analysis (Diniz-Filho, de Sant'Ana, & Bini, 1998; Diniz Filho, Bini, Sakamoto, & Brusatte, 2014).

First, the eigenvector of the time-calibrated oviraptorosaur phylogeny was extracted. Second, the S-component of each PC was extracted and tested for autocorrelation with Moran's I test to ensure the remaining phylogenetic signal is non-significant (Diniz Filho et al., 2014). If a significant phylogenetic signal was detected in the S-component (p-value <0.05), that PC was not included in the correlation test as we want to focus on detecting the correlation between size and skull forms without the potential influence of phylogenetic history. Thus, PC1 of the cranial form dataset was discarded. The S-components were regressed against centroid size (extracted from form datasets in MorphoJ (Klingenberg, 2011)) in R using the package 'PVR' (Santos, Diniz-Filho, e Luis, Bini, & Santos, 2018) to reveal the strength and significance of their correlations.

Form vs. function relationship

We performed three analyses to evaluate the correlation between mandibular function and form of different parts of the skull (Note S6; Table S6). Because of the differences in sample size between the form and function datasets, additional geometric morphometrics analyses and functional analyses were conducted to match the sample size for the correlation analysis, in order to make the two datasets maximally consistent for comparison. For example, 19 and 15 specimens are present in the lower beak form and mandibular function datasets, respectively. In this case, we conducted an extra 15-taxon geometric morphometric analysis for lower beak form. Following the same principle, five additional tests were conducted: an 8-taxon PCA of cranial form, a 9-taxon PCA of upper beak form, a 15-taxon PCA of lower beak form, an 8-taxon PCoA of mandibular function and a 9-taxon PCoA of mandibular function.

Non-phylogenetic methods were used to evaluate the overall relationship between form and function, which include two-block partial least squares (2B-PLS) analysis and multivariate multiple regression (MMR) analysis (Sakamoto, 2010) (Note S6). We also ultilised a phylogenetic method, PVR, to evaluate the form and function relationship. The S-components of the significant PC/PCO of each form dataset were extracted to remove any significant phylogenetic signal from influencing the results. The first two PCs and PCOs for each dataset were retained for correlation analyses between different form and function combinations (e.g. PC1 vs PCO1, PC1 vs PCO2 etc.; except the cranial form dataset). PC1 of the cranial form dataset was not included in the analysis as a significant phylogenetic signal remains in the S-component. See the electronic supplementary material section 6 for detailed methods.

Results

Morphological variation pattern

The analysis on the 11-taxon cranial dataset shows that PC1 mainly describes the anteroposterior length of the external naris, the depth of the premaxilla-maxilla region and the posterior extent of the maxilla (Figure S8). PC2 largely describes the relative position of the external naris, the anterior extent of the upper beak and the size of the orbit (Figure. S8). To a lesser extent, it also describes the length of the lateral temporal fenestra and the antorbital fenestra. The PC1 vs PC2 morphospace plot shows that the basal oviraptorosaur *Incisivosaurus* is separated from oviraptorids along both PC1 and PC2 (Figure 2A). (See the electronic supplementary material section 6 for full results.)

On the 15-taxon mandibular morphospace, PC1 largely describes the length and the height of the dentary, size of the external mandibular fenestra and the height of the coronoid process region (or the overall height of the mandible) (Figure S9). PC2 largely describes the posterior extent of the dorsal ramus of the dentary, the relative position of the external mandibular fenestra, the curvature of the ventral ramus of the dentary and the relative position of the articular glenoid (Figure. S9). The PC1 vs PC2 morphospace shows that oviraptorids and non-oviraptorids are separated along PC1 without any overlapping (Figure 2C). The non-oviraptorid taxa, caenagnathids and basal oviraptorosaurs, are separated from each other and the derived clades on PC2. The morphospace occupied by oviraptorids is visually much larger than that of caenagnathids.

On the 12-taxon upper beak morphospace, basal oviraptorosaurs are far separated from oviraptorids along PC1 (Figure 2B), as in the cranial PC plot. On the 19-taxon lower beak morphospace, PC1 largely separates the specimens into different taxonomic groups – oviraptorids, basal oviraptorosaurs and caenagnathids, from left to right (with exception of *Gigantoraptor*, which lies close to oviraptorids) (Figure 2D). The morphospace occupations of oviraptorids and caenagnathids slightly overlap, and they do not visually exhibit prominent differences in their areas.

NPMANOVA reveals that basal oviraptorosaurs exhibit significant morphospace separation compared to oviraptorids in the mandible form, upper beak form and lower beak form datasets (Table 1). However, there is no significant separation in the cranium form morphospace. When basal oviraptorosaurs are compared to caenagnathids, there are no significant differences in any of the morphospace-overlap comparisons. However, when caenagnathids are compared to oviraptorids, these groups are significantly separated in all morphospaces.

238 **Table 1**. Differences in morphospace occupation between major clade/grade of Oviraptorosauria
239 shown by NPMANOVA (p values; Bonferroni-corrected p-values (upper right)) (PC1-2/all sig
240 PC); significant p-values at $p<0.1$ ($0.05<p<0.1$) are underlined.

Compared groups	Form/function metric	p-value	Benjamini-Hochberg corrected p-value	
Basal oviraptorosaurs vs. oviraptorids	cranium form	0.1757/0.1801	0.1757/0.1801	
	mandible form	**0.0185/0.019**	**<u>0.02775/0.0285</u>**	
	upper beak form	**0.0139/0.0164**	**0.0139/0.0164**	
	lower beak form	**0.0232/0.0106**	**0.0348/0.0159**	
	mandible function	0.111/<u>0.0706</u>	0.1665/0.1059	
Basal oviraptorosaurs vs. caenagnathids	mandible form	<u>0.0696</u>/0.1321	0.06960/0.1321	
	lower beak form	0.6655/0.1967	0.6655/0.1967	
	mandible function	0.7349/0.1321	0.7349/0.1321	
Caenagnathids vs. oviraptorids	mandible form	**0.0011/ 0.0011**	**0.0033/0.0033**	
	lower beak form	**0.0007/0.0003**	**0.0021/0.0009**	

	mandible function	**0.0012/0.001**	**0.0036/0.0030**	

241

242

243

244 **Functional variation pattern**

245 In the 15-taxon dataset, there is no functional morphospace overlap between oviraptorids and other
246 oviraptorosaurs (Figure 3). Basal oviraptorosaurs and caenagnathids overlap in their functional
247 morphospaces, mainly because of the position of *Gigantoraptor* – which is closer to the oviraptorid
248 cluster than basal oviraptorosaurs along PCO1. Basal oviraptorosaurs and oviraptorids are
249 considerably spread out along PCO2, whereas caenagnathids are more restricted. Overall,
250 oviraptorids appear to occupy a larger functional morphospace than caenagnathids. (See electronic
251 supplementary material section 7 for complete results.)

252 NPMANOVA detected no significant difference in functional morphospace occupation between
253 basal oviraptorosaurs and caenagnathids/oviraptorids (Table 1). However, caenagnathids and
254 oviraptorids show significant morphospace separation, as in the mandibular and lower beak form
255 data sets.

256

257 **Evolution model of skull forms**

258 Blomberg's K test shows that there is no significant phylogenetic signal in any of the significant
259 PCs of the cranium matrix (Table 2 & S14). However, we find a significant and strong

phylogenetic signal in PC1 but not in any other PCs of the mandible and upper beak datasets. In contrast, PC1 of the lower beak form dataset shows a weak but significant phylogenetic signal (K, 0.565; p-value, 0.002), while no phylogenetic signal was detected in PC2.

The permutation test reveals that the overall shape of the oviraptorosaur cranium is not significantly correlated with phylogeny (Table S15). The overall shape of the oviraptorosaur mandible, upper beak and lower beak, however, are significantly correlated with phylogeny.

278 **Table 2**. Phylogenetic signal in the morphometric data shown by Blomberg's K test (see Table
279 S14 for full results).

Data	PC	K	PIC.var.obs	PIC.var.rnd.mean	p-value	Benjamini-Hochberg corrected p-value	PIC.var.Zscore
Cranium	PC1	0.850	0.000357	0.000320	0.71	0.902	0.283
Mandible	PC1	**2.203**	0.000329	0.00165	**0.001**	**0.006**	-3.448
Upper beak	PC1	**3.243**	0.000611	0.00150	**0.009**	**0.027**	-1.728
Lower beak	PC1	**0.565**	0.00176	0.00656	**0.001**	**0.003**	-2.117

280
281
282
283
284
285
286
287
288

289 **Allometry**

290 Regressions reveal no significant correlation between the S-component of PC scores and centroid
291 sizes in any of the significant form PC (Table. S16). This implies that none of the significant PC
292 variations are primarily allometric in nature. However, it is worth-noting that PC1 of lower beak
293 form shows moderate correlation with specimen size ($p=0.08665$; corrected $p=0.25995$).

294

295 **Form and function relationship**

296 2B-PLS analysis reveals no significant correlation between cranial form and mandibular function,
297 but significant correlations between the mandible, upper beak and lower beak when each are
298 compared to mandibular function (Table S17). No significant correlation is detected in MMR
299 analysis between cranium form and mandibular function (Table S18). MMR analyses using
300 different test statistics consistently show that mandible/lower beak form is significantly correlated
301 with mandibular function. Although MMR analyses reveal that the upper beak has strong
302 correlations with function, all the test statistics suggest these correlations to be non-significant,
303 except Pillai's trace.

304 PVR on form and function shows that cranium PC2 does not have a significant correlation with
305 function PCO1 and PCO2 (Table 3 & S19). No significant correlation is found between the upper
306 beak and functional dataset, either. Both PC1 of the mandible and lower beak show a significant
307 correlation with function PCO1. In comparison, the correlation between lower beak and function
308 is slightly stronger and more significant than the one between mandible and function. PC1 of the
309 lower beak also shows a significant correlation with function PCO2.

310

311 **Table 3**. Correlation between form and function shown by phylogenetic eigenvector regression
312 (PVR) correlation test (see Table S19 for full results).

Form	Correlation pairs	Coefficient of determination (R^2)	p-value	Benjamini-Hochberg corrected p-value
Cranium	PC2c vs PCO1fc	0.0113	0.802	0.954
	PC2c vs PCO2fc	0.000616	0.954	0.954
Mandible	PC1m vs PCO1fm	0.506	**0.00292**	**0.0117**
	PC1m vs PCO2fm	0.193	0.101	0.127
Upper beak	PC1p vs PCO1fp	0.190	0.240	0.321
	PC1p vs PCO2fp	0.0437	0.590	0.590
Lower beak	PC1d vs PCO1fd	0.535	**0.00195**	**0.00780**
	PC1d vs PCO2fd	0.273	**0.0456**	0.0911

313
314
315
316
317
318
319

Discussion

Diversification of oviraptorosaur skull form

The cranial form of oviraptorosaurs mainly varies in the snout region (premaxilla and maxilla). Overall, the modified snouts of oviraptorids are downturned compared to those of basal oviraptorosaurs: the dorsal margin of the jugal-quadratojugal and the dorsal margin of the premaxilla form an obtuse angle in lateral view. It seems reasonable that this difference implies different cranial mechanics. For example, a more inclined beak was found to be correlated with bite force increase in finches (van der Meij & Bout, 2008). Thus, the downturned snout of oviraptorids may have been an adaptation for a powerful bite. Large variation in the shape, size and relative position of the external naris is also detected, which is perhaps related to the observed modification of snout orientation (PC1 & 2; Figure S8) (Lü, Chen, Brusatte, Zhu, & Shen, 2016; Lü et al., 2015). However, the implications of the high variability in naris shape are more difficult to explain, as the nasal region of vertebrates is related to a variety of biological roles (i.e. sound production, olfactory and respiratory) (Witmer, 2001). It is also possible that the variable external naris is a by-product of the development of a prominent cranial crest in some oviraptorosaurs, which was likely a socio-display structure (Lü et al., 2017). If this is the case, then the variation in the naris region may not imply any particular biomechanical variation among oviraptorosaurs.

The mandible and lower beak form datasets include specimens of basal oviraptorosaurs, caenagnathids and oviraptorids, allowing us to assess large-scale form variations between these major groups. The wide separation between caenagnathids and oviraptorids in the mandible form morphospace is not surprising, as their differences in mandibular anatomy are well-noted (Funston et al., 2015; Funston, Mendonca, Currie, & Barsbold, 2017; Longrich, Barnes, Clark, & Millar,

2013; Longrich, Currie, & Dong, 2010; Ma et al., 2017; Osmolska et al., 2004). The lower beak form morphospace also displays a similar pattern, with most caenagnathids and oviraptorids situated at the opposing sides and basal oviraptorosaurs located between them on PC1. However, in both morphospaces, *Gigantoraptor* is located closer to oviraptorids than other caenagnathids and even basal oviraptorosaurs on PC1, despite phylogenetic studies consistently placing it within caenagnathids (Longrich et al., 2013; Lü et al., 2017; Yu et al., 2018). The functional morphospace shows a similar pattern with that of mandible form, as caenagnathids and oviraptorids are separated on PC1 and do not overlap. Similarly, *Gigantoraptor* is positioned close to the oviraptorid cluster. These results indicate that *Gigantoraptor* evolved a more oviraptorid-like mandible form that deviates from those of other caenagnathids, which perhaps relates to an allometric effect and/or a unique feeding style suitable for its gigantic body size (Ma et al., 2017).

Overall, the largest variation among oviraptorosaur skulls is in the rostral portion: PCs1 of the cranium and mandible datasets mainly describe variation in the snout region and the dentary region, respectively (Figures S8 & S9). Large-scale geometric morphometric studies on theropods (Brusatte et al., 2012; Foth & Rauhut, 2013) and extant birds (Marugán-Lobón & Buscalioni, 2006) have consistently identified the snout to be highly variable compared to other parts of the cranium. Some studies focusing on particular extant bird families also found substantial cranial variation in the beak region (Grant & Grant, 1996; Kulemeyer, Asbahr, Gunz, Frahnert, & Bairlein, 2009; Sun, Si, Wang, Wang, & Zhang, 2018). Our results demonstrate that this pattern still persists within a restricted taxonomic theropod group like oviraptorosaurs, despite the development of highly modified skull forms that deviate from those of other theropods (Brusatte et al., 2012; Foth & Rauhut, 2013).

365 **Phylogenetic signals in oviraptorosaur skull forms**

366 There are several possible interpretations for why we did not find any phylogenetic signal in the
367 shape of the cranium. Oviraptorosaur skull shape may have evolved under various different
368 selection pressures. For instance, selection on feeding mechanics, olfaction, vision, intelligence,
369 and sexual display (e.g., cranial crest) may affect skull shape evolution in wildly different ways,
370 with the combined effect being a departure from Brownian motion in the evolution of skull shape.
371 It is possible that phenotypic proxies for these individual selection pressures may show
372 phylogenetic signals on their own. This is supported by the upper beak analysis, as this region
373 shows strong phylogenetic signal (K>3) while being part of the cranium, indicating that at least
374 one cranial region evolved under potentially strong stabilizing selection (K>1 implies strong
375 phylogenetic conservatism or weaker tendency to deviate away from the ancestral shape).
376 Alternatively, failure to detect phylogenetic signal in the overall cranial shape dataset may be
377 because of a lack of statistical power owing to small sample size (N=11). Because morphometric
378 studies encompassing a wide range of non-avian theropods have detected a high phylogenetic
379 signal in their cranial morphologies, our results indicate that such signals may be weaker within
380 subclades (Brusatte et al., 2012; Foth & Rauhut, 2013).

381 That mandible and upper beak forms both have significant and strong phylogenetic signals – with
382 K>1 –indicates that these cranio-mandibular regions are more phylogenetically 'conserved' than
383 expected under Brownian motion. That is, closely related taxa are more similar in shape than
384 expected given the branch lengths. Interestingly, the K < 1 in lower beak form indicates that a
385 large proportion of lower beak shape variance cannot be explained by Brownian motion evolution
386 alone – i.e., closely related taxa are more disparate in shape than expected given branch length –
387 and may be indicative of additional processes like adaptive evolution or directional evolution

388 (Blomberg et al., 2003) as well as the possibility of noise in the data. The discrepancy in K between
389 different parts of the skull indicates that the skull of oviraptorosaurs is not a single, well-integrated
390 structure. A certain part, in this case the shape changes associated with PC1 in the lower beak
391 (length and depth of the beak), may have been governed by an evolutionary process that is distinct
392 from the other parts of the skull/mandible.

393

394 **Correlation of oviraptorosaur skull forms and mandible function**

395 Our findings that cranium and upper beak forms (the latter once accounting for phylogeny) show
396 no significant relationships with mandibular function is consistent with previous studies (Brusatte
397 et al., 2012; Foth & Rauhut, 2013). However, on the contrary, we find significant relationships
398 between mandible and lower beak forms and mandibular functions. The discrepancy in form-
399 function relationships between the skull and mandible can possibly be explained by the fact that
400 the cranium has multiple functional roles (e.g. feeding, neurosensory and social display etc.)
401 whereas the role of the mandible is less variable (i.e. feeding). Thus, a single function is not capable
402 of explaining the variance in skull shape but can do so for mandible shape. However, a study on
403 herbivorous dinosaurs suggests that morphologically similar skulls could have disparate functional
404 properties, as demonstrated by 3D biomechanical techniques like finite element analysis and bite
405 force estimation (Lautenschlager, Brassey, Button, & Barrett, 2016). It is possible that future in-
406 depth 3D biomechanical studies would demonstrate a similar pattern in oviraptorosaur mandibles.
407 If the close association between form and function is supported by future analysis, this would
408 consolidate our finding that feeding mechanics likely played an important role in shaping the
409 mandible and the lower beak of oviraptorosaurs.

410 **Beak evolution**

411 One of the most fascinating features of derived oviraptorosaur skulls is the presence of a toothless
412 beak (Balanoff & Norell, 2012; Ma et al., 2017; Osmolska et al., 2004) . Different levels of tooth
413 reduction are known among non-avian dinosaurs (Zanno & Makovicky, 2011), but only some
414 oviraptorosaurs, some ornithomimosaurs and mature *Limusaurus* exhibit complete tooth loss as in
415 extant birds (Makovicky, Kobayashi, & Currie, 2004; Osmolska et al., 2004; Xu et al., 2009). The
416 beak shape of extant birds is usually regarded as closely associated with diet (Grant & Grant, 1996;
417 Grant & Grant, 2006). However, recent studies demonstrate that a number of other factors may
418 also play a role in influencing beak shape, such as phylogeny, size and function (i.e. mechanical
419 advantage) (Bright et al., 2016; Navalón, Bright, Marugán-Lobón, & Rayfield, 2018; Shao et al.,
420 2016). Our results show that oviraptorosaur lower beak shape is in general closely related to
421 phylogeny and function, as in mandible form. Interestingly, a moderate allometric signal is
422 detected in lower beak form (R^2=0.162852; p=0.08665; corrected p=0.25995). Together, these
423 findings may suggest that the mechanisms governing beak shape in birds are similar to those in
424 oviraptorosaurs, despite the independent evolution of a toothless beak in these two clades.

425

426 **Niche partitioning between major clades of oviraptorosaurs**

427 Previous studies have noted a number of function-related anatomical dissimilarities between
428 caenagnathids and oviraptorids (Funston et al., 2015; Longrich et al., 2013; Ma et al., 2017). In
429 our study, these two clades are significantly separated from each other in both morphological and
430 functional morphospace, as revealed by NPMANOVA. Eight functional characters are considered
431 to have a significant contribution to functional PCO1 variations (Table S13). These characters

include proxies for mechanical advantage, jaw robustness and occlusal mode (Note S1). The large separation between caenagnathids and oviraptorids in functional morphospace likely indicates that they had distinct feeding styles, corroborating previous suggestions based on comparative anatomy (Funston et al., 2015; Longrich et al., 2013; Longrich et al., 2010; Ma et al., 2017; Smith, 1992). Our results also provide quantitative support to the hypothesis that caenagnathids and oviraptorids coexisted through niche-partitioning in the Mongolian Nemegt Formation ecosystem (Funston et al., 2017), and probably other ecosystems as well. Toothed basal oviraptorosaurs likely shared similar jaw mechanics as caenagnathids because they have a number of anatomical similarities (Wang et al., 2018). The NPMANOVA tests reinforce this idea by demonstrating that basal oviraptorosaurs are not significantly separated from caenagnathids in the various morphospaces, but often are significantly separated from oviraptorids. Taken together, these results suggest that oviraptorids are a highly derived clade which developed unique mandible morphologies distinctive from other oviraptorosaurs.

Niche partitioning within caenagnathids and oviraptorids

The diverse mandibular function of oviraptorids has likely allowed some of them to partition feeding niches in the same ecosystem. The Late Cretaceous Nanxiong Formation in the Ganzhou region of Jiangxi, China, is the best example of within-clade co-occurrence of multiple oviraptorosaur species (Lü et al., 2017). Since 2010, seven new oviraptorids have been described from this formation (Lü et al., 2016; Lü et al., 2017; Lü et al., 2015; Lü, Yi, Zhong, & Wei, 2013; Wang, Sun, Sullivan, & Xu, 2013; Wei, Pu, Xu, Liu, & Lu, 2013; Xu & Han, 2010), leading researchers to propose that these species diversified during an evolutionary radiation, perhaps driven by differences in feeding style (Lü et al., 2016). Our results show that the Ganzhou taxa

occupy a wide spread in both morphological and functional spaces (Figures. 2 & 3), instead of clustering together, supporting the hypothesis that their coexistence was facilitated by dietary-related niche-partitioning (see electronic supplementary material section 14).

Caenagnathids might have partitioned niches as well, but with a different strategy: they developed a wide range of body sizes (Yu et al., 2018). In the Nei Mongol Erlian Formation, *Gigantoraptor*, the largest known caenagnathid, has a mandible length and dentary width of 46.0 cm and 10.0 cm, respectively (Ma et al., 2017). In contrast, *Caenagnathasia*, a small caenagnathid from the same ecosystem, has a dentary width of 1.56 cm (Yao et al., 2015). By having different jaw sizes, caenagnathids could have procured different types of food, and hence developed varying feeding strategies (Ma et al., 2017). It is likely that derived oviraptorosaurs – caenagnathids and oviraptorids – developed different intra-clade niche-partitioning strategies to reduce competition among themselves. The high ecological variability of derived oviraptorosaurs—underpinned by their cranial and mandibular form and functional variations—might have been key to their diversification in the Late Cretaceous, and their important role in the last pre-extinction dinosaur ecosystems of the northern hemisphere.

References

Balanoff, A. M., & Norell, M. A. (2012). Osteology of Khaan mckennai (Oviraptorosauria: Theropoda). *Bulletin of the American Museum of Natural History*(372), 1-76.

Blomberg, S. P., Garland, T., & Ives, A. R. (2003). Testing for phylogenetic signal in comparative data: behavioral traits are more labile. *Evolution, 57*(4), 717-745.

Bright, J. A., Marugán-Lobón, J., Cobb, S. N., & Rayfield, E. J. (2016). The shapes of bird beaks are highly controlled by nondietary factors. *Proceedings of the National Academy of Sciences*, 201602683.

Brusatte, S. L., Sakamoto, M., Montanari, S., Harcourt, S., & William, E. H. (2012). The evolution of cranial form and function in theropod dinosaurs: insights from geometric morphometrics. *Journal of evolutionary biology, 25*(2), 365-377.

Diniz-Filho, J., Alves, D., Villalobos, F., Sakamoto, M., Brusatte, S., & Bini, L. (2015). Phylogenetic eigenvectors and nonstationarity in the evolution of theropod dinosaur skulls. *Journal of evolutionary biology, 28*(7), 1410-1416.

Diniz-Filho, J. A. F., de Sant'Ana, C. E. R., & Bini, L. M. (1998). An eigenvector method for estimating phylogenetic inertia. *Evolution, 52*(5), 1247-1262.

Diniz Filho, J. A. F., Bini, L. M., Sakamoto, M., & Brusatte, S. L. (2014). Phylogenetic eigenvector regression in paleobiology.

Foth, C., & Rauhut, O. W. (2013). Macroevolutionary and morphofunctional patterns in theropod skulls: a morphometric approach. *Acta Palaeontologica Polonica, 58*(1), 1-16.

Funston, G. F., & Currie, P. J. (2014). A previously undescribed caenagnathid mandible from the late Campanian of Alberta, and insights into the diet of Chirostenotes pergracilis (Dinosauria: Oviraptorosauria). *Canadian Journal of Earth Sciences, 51*(2), 156-165.

Funston, G. F., Currie, P. J., & Burns, M. E. (2015). New elmisaurine specimens from North America and their relationship to the Mongolian Elmisaurus rarus. *Acta Palaeontologica Polonica*.

Funston, G. F., Mendonca, S. E., Currie, P. J., & Barsbold, R. (2017). Oviraptorosaur anatomy, diversity and ecology in the Nemegt Basin. *Palaeogeography, Palaeoclimatology, Palaeoecology*.

Grant, B. R., & Grant, P. R. (1996). High survival of Darwin's finch hybrids: effects of beak morphology and diets. *Ecology, 77*(2), 500-509.

Grant, P. R., & Grant, B. R. (2006). Evolution of character displacement in Darwin's finches. *Science, 313*(5784), 224-226.

Hammer, Ø., Harper, D., & Ryan, P. (2001). PAST: Paleontological Statistics software package for education and data analysis. *Palaeontologia Electronica, 4*(1), 1-9.

Ji, Q., Currie, P. J., Norell, M. A., & Ji, S. A. (1998). Two feathered dinosaurs from northeastern China. *Nature, 393*(6687), 753-761.

Ji, Q., Lü, J., Wei, X., & Wang, X. (2012). A new oviraptorosaur from the Yixian Formation of Jianchang, western Liaoning Province, China. *Geological Bulletin of China, 31*, 2102-2107.

Kembel, S. W., Cowan, P. D., Helmus, M. R., Cornwell, W. K., Morlon, H., Ackerly, D. D., . . . Webb, C. O. (2010). Picante: R tools for integrating phylogenies and ecology. *Bioinformatics, 26*(11), 1463-1464.

Klingenberg, C. P. (2011). MorphoJ: an integrated software package for geometric morphometrics. *Molecular ecology resources, 11*(2), 353-357.

Kulemeyer, C., Asbahr, K., Gunz, P., Frahnert, S., & Bairlein, F. (2009). Functional morphology and integration of corvid skulls–a 3D geometric morphometric approach. *Frontiers in Zoology, 6*(1), 2.

Laurin, M. (2004). The evolution of body size, Cope's rule and the origin of amniotes. *Systematic biology, 53*(4), 594-622.

Lautenschlager, S., Brassey, C. A., Button, D. J., & Barrett, P. M. (2016). Decoupled form and function in disparate herbivorous dinosaur clades. *Scientific Reports, 6*, 26495.

523 Lee, S., Lee, Y.-N., Chinsamy, A., Lü, J., Barsbold, R., & Tsogtbaatar, K. (2019). A new baby
524 oviraptorid dinosaur (Dinosauria: Theropoda) from the Upper Cretaceous Nemegt
525 Formation of Mongolia. *PLoS ONE, 14*(2), e0210867.
526 Longrich, N. R., Barnes, K., Clark, S., & Millar, L. (2013). Caenagnathidae from the Upper
527 Campanian Aguja Formation of West Texas, and a Revision of the Caenagnathinae.
528 *Bulletin of the Peabody Museum of Natural History, 54*(1), 23-49.
529 Longrich, N. R., Currie, P. J., & Dong, Z. (2010). A new oviraptorid (Dinosauria: Theropoda)
530 from the Upper Cretaceous of Bayan Mandahu, Inner Mongolia. *Palaeontology, 53*(5),
531 945-960.
532 Lü, J., Chen, R., Brusatte, S. L., Zhu, Y., & Shen, C. (2016). A Late Cretaceous diversification
533 of Asian oviraptorid dinosaurs: evidence from a new species preserved in an unusual
534 posture. *Scientific Reports, 6*.
535 Lü, J., Currie, P. J., Xu, L., Zhang, X., Pu, H., & Jia, S. (2013). Chicken-sized oviraptorid
536 dinosaurs from central China and their ontogenetic implications. *Naturwissenschaften,*
537 *100*(2), 165-175.
538 Lü, J., Li, G., Kundrát, M., Lee, Y.-N., Sun, Z., Kobayashi, Y., . . . Liu, H. (2017). High diversity
539 of the Ganzhou Oviraptorid Fauna increased by a new "cassowary-like" crested species.
540 *Scientific Reports, 7*(1), 6393.
541 Lü, J., Pu, H., Kobayashi, Y., Xu, L., Chang, H., Shang, Y., . . . Shen, C. (2015). A New
542 Oviraptorid Dinosaur (Dinosauria: Oviraptorosauria) from the Late Cretaceous of
543 Southern China and Its Paleobiogeographical Implications. *Scientific Reports, 5*.
544 doi:10.1038/srep11490
545 Lü, J., Yi, L., Zhong, H., & Wei, X. (2013). A new oviraptorosaur (Dinosauria:
546 Oviraptorosauria) from the Late Cretaceous of southern China and its paleoecological
547 implications. *PLoS ONE, 8*(11), e80557.
548 Ma, W., Wang, J., Pittman, M., Tan, Q., Tan, L., Guo, B., & Xu, X. (2017). Functional anatomy
549 of a giant toothless mandible from a bird-like dinosaur: *Gigantoraptor* and the evolution
550 of the oviraptorosaurian jaw. *Scientific Reports, 7*, 16247.
551 Makovicky, P. J., Kobayashi, Y., & Currie, P. J. (2004). Ornithomimosauria. *The Dinosauria, 2*,
552 137-150.
553 Marugán-Lobón, J., & Buscalioni, Á. D. (2006). Avian skull morphological evolution: exploring
554 exo-and endocranial covariation with two-block partial least squares. *Zoology, 109*(3),
555 217-230.
556 Navalón, G., Bright, J. A., Marugán-Lobón, J., & Rayfield, E. J. (2018). The evolutionary
557 relationship among beak shape, mechanical advantage, and feeding ecology in modern
558 birds. *Evolution*.
559 Osmolska, H., Currie, P. J., & Barsbold, R. (2004). Oviraptorosauria. In D. B. Weishampel, P.
560 Dodson, & H. Osmolska (Eds.), *The Dinosauria* (Second ed., pp. 165-183): University of
561 California Press.
562 Pu, H., Zelenitsky, D. K., Lü, J., Currie, P. J., Carpenter, K., Xu, L., . . . Chuang, H. (2017).
563 Perinate and eggs of a giant caenagnathid dinosaur from the Late Cretaceous of central
564 China. *Nature Communications, 8*, 14952.
565 Rohlf, F. (2017). tpsDig, version 1.74. http://life.bio.sunysb.edu/morph/index.html.
566 Sakamoto, M. (2010). Jaw biomechanics and the evolution of biting performance in theropod
567 dinosaurs. *Proceedings of the Royal Society B: Biological Sciences, 277*(1698), 3327-
568 3333.

569 Santos, T., Diniz-Filho, J. A., e Luis, T. R., Bini, M., & Santos, M. T. (2018). Package 'PVR'.
570 Shao, S., Quan, Q., Cai, T., Song, G., Qu, Y., & Lei, F. (2016). Evolution of body morphology
571 and beak shape revealed by a morphometric analysis of 14 Paridae species. *Frontiers in*
572 *Zoology, 13*(1), 30.
573 Smith, D. (1992). The type specimen of Oviraptor philoceratops, a theropod dinosaur from the
574 Upper Cretaceous of Mongolia. *Neues Jahrbuch für Geologie und Paläontologie*
575 *Abhandlungen, 186*(3), 365-388.
576 Sun, Y., Si, G., Wang, X., Wang, K., & Zhang, Z. (2018). Geometric morphometric analysis of
577 skull shape in the Accipitridae. *Zoomorphology*, 1-12.
578 Tokita, M., Yano, W., James, H. F., & Abzhanov, A. (2017). Cranial shape evolution in adaptive
579 radiations of birds: comparative morphometrics of Darwin's finches and Hawaiian
580 honeycreepers. *Phil. Trans. R. Soc. B, 372*(1713), 20150481.
581 van der Meij, M. A., & Bout, R. G. (2008). The relationship between shape of the skull and bite
582 force in finches. *Journal of Experimental Biology, 211*(10), 1668-1680.
583 Wang, S., Stiegler, J., Wu, P., Chuong, C.-M., Hu, D., Balanoff, A., . . . Xu, X. (2017).
584 Heterochronic truncation of odontogenesis in theropod dinosaurs provides insight into the
585 macroevolution of avian beaks. *Proceedings of the National Academy of Sciences,*
586 *114*(41), 10930-10935.
587 Wang, S., Sun, C., Sullivan, C., & Xu, X. (2013). A new oviraptorid (Dinosauria: Theropoda)
588 from the Upper Cretaceous of southern China. *Zootaxa, 3640*(2), 242-257.
589 Wang, S., Zhang, Q., & Yang, R. (2018). Reevaluation of the dentary structures of caenagnathid
590 oviraptorosaurs (Dinosauria, Theropoda). *Scientific Reports, 8*(1), 391.
591 Wei, X., Pu, H., Xu, L., Liu, D., & Lu, J. (2013). A New Oviraptorid Dinosaur (Theropoda:
592 Oviraptorosauria) from the Late Cretaceous of Jiangxi Province, Southern China. *Acta*
593 *Geologica Sinica-English Edition, 87*(4), 899-904. doi:10.1111/1755-6724.12098
594 Witmer, L. M. (2001). Nostril position in dinosaurs and other vertebrates and its significance for
595 nasal function. *Science, 293*(5531), 850-853.
596 Xu, X., Cheng, Y., Wang, X., & Chang, C. (2002). An unusual oviraptorosaurian dinosaur from
597 China. *Nature, 419*.
598 Xu, X., Clark, J. M., Mo, J., Choiniere, J., Forster, C. A., Erickson, G. M., . . . Nesbitt, S. (2009).
599 A Jurassic ceratosaur from China helps clarify avian digital homologies. *Nature,*
600 *459*(7249), 940.
601 Xu, X., & Han, F.-L. (2010). A new oviraptorid dinosaur (Theropoda: Oviraptorosauria) from
602 the Upper Cretaceous of China. *Vertebrata Palasiatica, 48*(1), 11-18.
603 Yao, X., Wang, X.-L., Corwin, S., Wang, S., Stidham, T., & Xu, X. (2015). Caenagnathasia sp
604 (Theropoda: Oviraptorosauria) from the Iren Dabasu Formation (Upper Cretaceous:
605 Campanian) of Erenhot, Nei Mongol, China. *Vertebrata Palasiatica, 53*(4), 291-298.
606 Yu, Y., Wang, K., Chen, S., Sullivan, C., Wang, S., Wang, P., & Xu, X. (2018). A new
607 caenagnathid dinosaur from the Upper Cretaceous Wangshi Group of Shandong, China,
608 with comments on size variation among oviraptorosaurs. *Scientific Reports, 8*(1), 5030.
609 Zanno, L. E., & Makovicky, P. J. (2011). Herbivorous ecomorphology and specialization
610 patterns in theropod dinosaur evolution. *Proceedings of the National Academy of*
611 *Sciences, 108*(1).

612

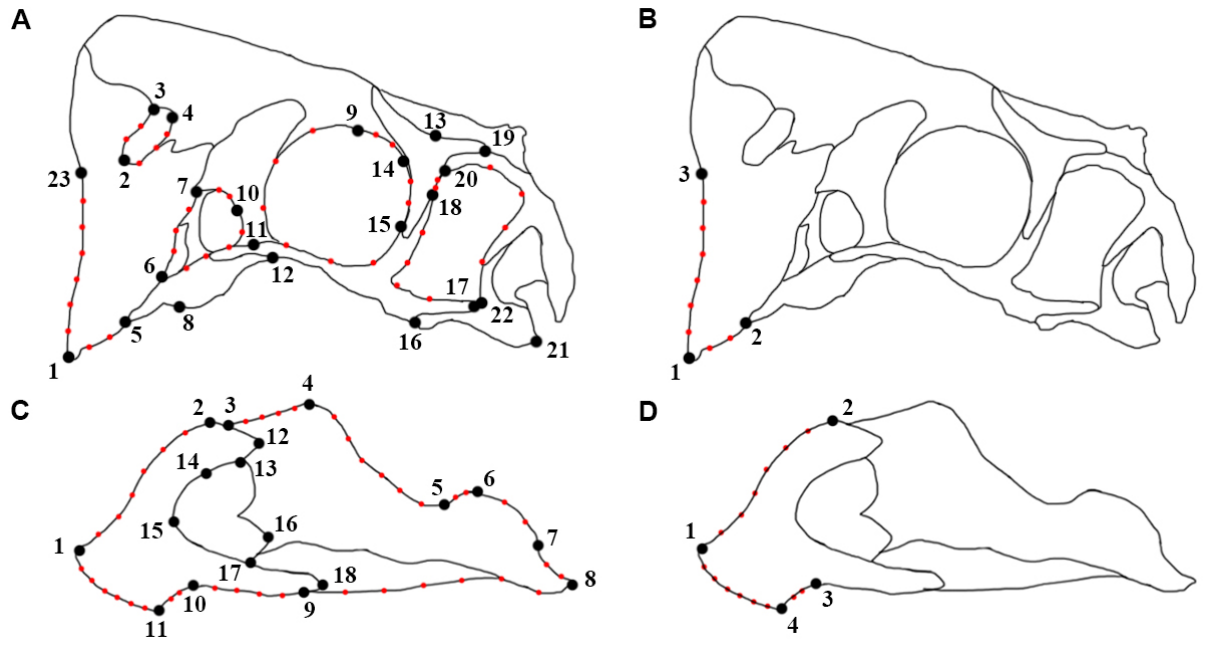

Figure 1. Homologous landmarks plotted on the (a) cranium, (b) upper beak, (c) mandible and (d) lower beak of oviraptorosaurs for geometric morphometric analysis. Black dots indicate fixed landmarks; red dots indicate semi-landmarks. See Tables S2-5 for descriptions of landmarks.

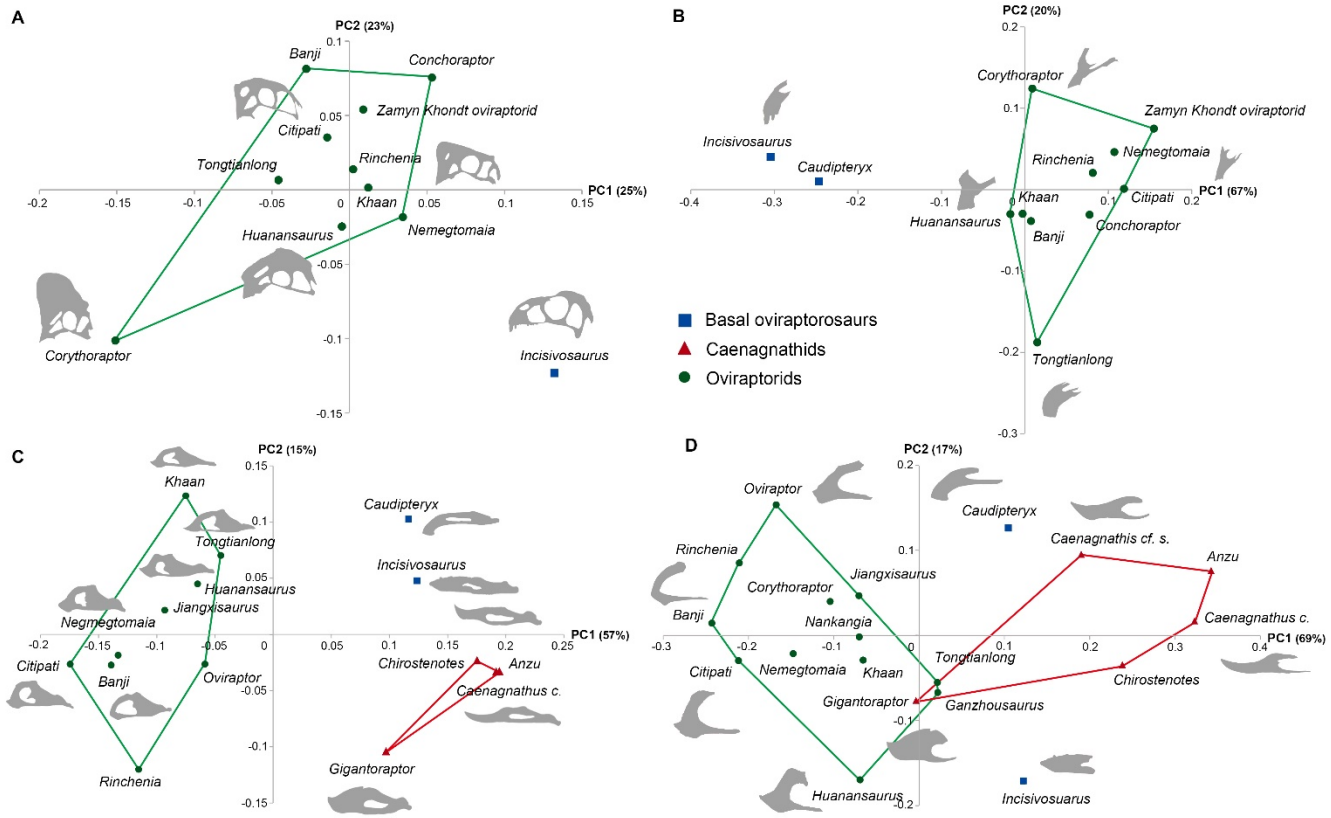

Figure 2. Two-dimensional morphospaces of oviraptorosaur skull form dataset. (A) Cranial morphospace of the 11-taxon dataset; (B) Upper beak morphospace of the 12-taxon dataset; (C) Mandibular morphospace of the 15-taxon dataset and (D) Lower beak morphospace of the 19-taxon dataset. Each morphospace depicts the first PCA axis versus the second axis. See Table S1 for sources of the images used.

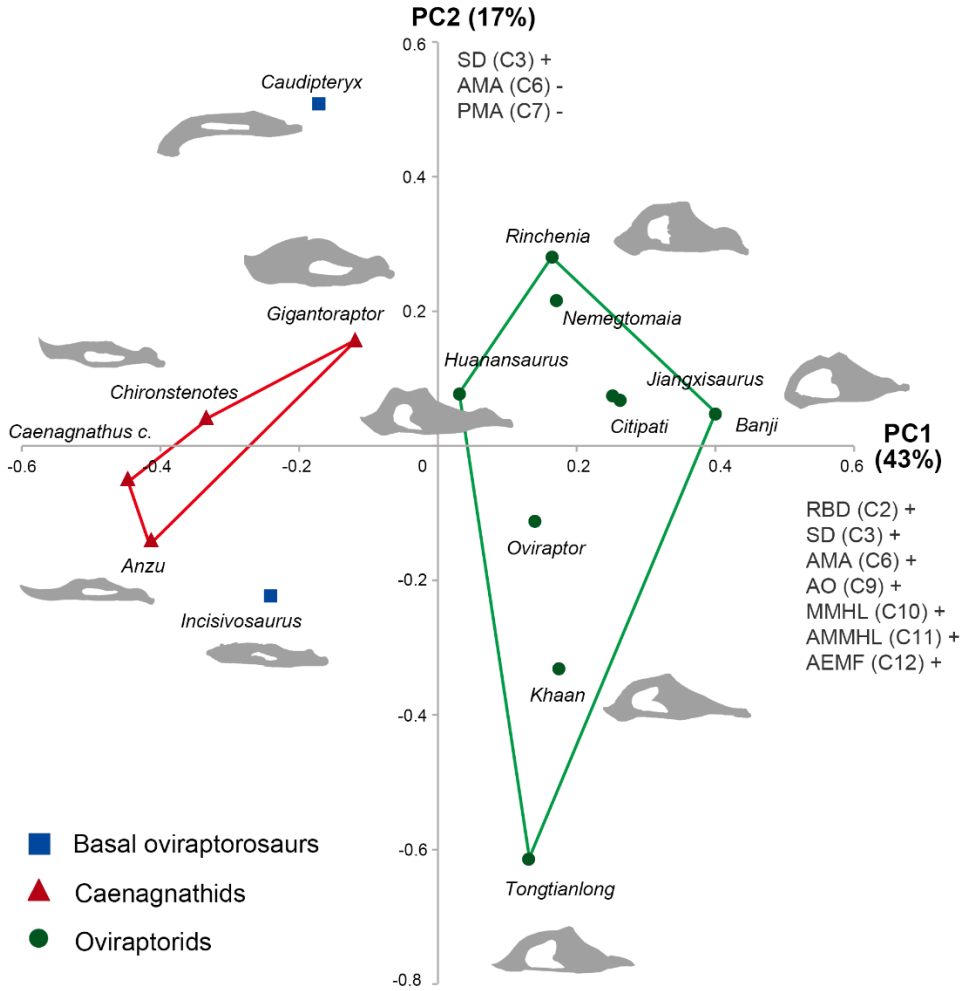

635

636 **Figure 3. Two-dimensional functional morphospace of the 15-taxon mandibular function**
637 **dataset.** AEMF, relative area of external mandibular fenestra; AMA, anterior mechanical
638 advantage; AMMHL, average mandibular height; AO, articular offset; MMHL, maximum
639 mandibular height; PMA, posterior mechanical advantage; RBD, relative beak depth; SD,
640 symphysis deflection.

641

642

Acknowledgements

WM thanks David Button for his comments that greatly improve this study and Stephan Lautenschlager for his comments on the manuscript. SLB thanks his good friend, the late JL, for many years of collaboration and camaraderie. MS thanks Chris Venditti, Andrew Meade, and George Butler for invaluable discussion. SLB's work in China on Ganzhou oviraptorids was funded by a Marie Curie Career Integration Grant (EC 630652) and the University of Edinburgh, and his lab is supported by ERC StG 'PalM' (European Research Council [ERC] under the European Union's Horizon 2020 Research and Innovation Programme; Grant number: 756226). JL was supported by the National Natural Science Foundation of China (grant Nos 41672019 and 41688103). MS was supported by the Leverhulme Trust (RPG-2017-071).

Supporting information

Table S1. List of taxon and specimens included in the geometric morphometric analysis and functional analysis.

Table S2. Homologous landmarks on oviraptorosaur cranium.

Table S3. Homologous landmarks on oviraptorosaur mandible.

Table S4. Homologous landmark on oviraptorosaur upper beak.

Table S5. Homologous landmark on oviraptorosaur lower beak.

Table S6. Specimens included in geometric morphometric analysis and functional analysis for each data sets.

Table S7. First occurrence of oviraptorosaur specimens.

Table S8. Morphological variation of the 11-taxon cranium form data set explained by the first 10 PCA axes.

Table S9. Morphological variation of the 15-taxon mandible form data set explained by the first 14 PCA axes.

Table S10. Morphological variation of the 12-taxon upper beak form data set explained by the first 11 PCA axes.

Table S11. Morphological variation of the 19-taxon lower beak form data set explained by the first 18 PCA axes.

Table S12. Functional variation of the 15-taxon mandibular function data set explained by the first 13 PCO axes.

686 **Table S13**. Correlations between functional characters and the first 2 PCO axes.

687 **Table S14**. Phylogenetic signal in the morphometric data shown by Blomberg's K test.

688 **Table S15**. Phylogenetic signal in the morphometric data shown by permutation test.

689 **Table S16**. Allometric signal in the morphological data shown by regression analysis between
690 forms and specimen size (represented by centroid size).

691 **Table S17**. Correlation between form and function shown by two-block partial least squares (2B-
692 PLS) analysis.

693 **Table S18**. Correlation between form and function shown by multivariate multiple regression
694 (MMR) analysis.

695 **Table S19**. Correlation between form and function shown by phylogenetic eigenvector regression
696 (PVR) correlation test.

697 **Table S20**. Morphological variation of the 8-taxon cranium form data set explained by the first 7
698 PCA axes.

699 **Table S21**. Morphological variation of the 9-taxon upper beak form data set explained by the first
700 8 PCA axes.

701 **Table S22**. Morphological variation of the 15-taxon lower beak form data set explained by the
702 first 14 PCA axes.

703 **Table S23**. Functional variation of the 8-taxon mandibular function data set explained by the first
704 8 PCO axes.

705 **Table S24**. Functional variation of the 9-taxon mandibular function data set explained by the first
706 9 PCO axes

707 **Table S25**. Landmarks representing different mandible sections.

708 **Table S26**. Correlation between mandible sections and overall morphology of mandible shown by
709 two-block partial least squares (2B-PLS) analysis **Table S27**. Disparity analysis comparing the
710 forms and function of caenagnathids and oviraptorids.

711 **Table S28**. Disparity analysis comparing the forms and function of Ganzhou oviraptorosaurs and
712 non-Ganzhou oviraptorosaurs.

713 **Table S29**. Disparity analysis comparing the forms and function of Ganzhou oviraptorids and non-
714 Ganzhou oviraptorids.

715 **Figure S1**. Homologous landmarks plotted on the (a) cranium and (b) mandible of oviraptorosaurs
716 for geometric morphometric analysis.

717 **Figure S2**. Homologous landmarks plotted on the (a) upper beak and (b) lower beak of
718 oviraptorosaurs for geometric morphometric analysis.

719 **Figure S3**. Phylogenetic trees of Oviraptorosauria used in this study.

720 **Figure S4**. Two-dimensional morphospaces with phylogenetic tree mapped for the 11-taxon
721 cranium form data set.

722 **Figure S5**. Two-dimensional morphospaces with phylogenetic tree mapped for the 15-taxon
723 mandible form data set.

724 **Figure S6**. Two-dimensional morphospaces with phylogenetic tree mapped for the 12-taxon upper
725 beak form data set.

726 **Figure S7**. Two-dimensional morphospaces with phylogenetic tree mapped for the 19-taxon lower
727 beak form data set.

728 **Figure S8**. Major shape changes in cranium based on 11-taxon data set.

729 **Figure S9**. Major shape changes in mandible based on 15-taxon data set.

730 **Figure S10**. Major shape changes in upper beak based on 12-taxon data set.

731 **Figure S11**. Major shape changes in lower beak based on 19-taxon data set.

732 **Figure S12**. Two-dimensional morphospaces with phylogenetic tree mapped for the 8-taxon
733 cranium form data set.

734 **Figure S13**. Two-dimensional morphospaces with phylogenetic tree mapped for the 9-taxon upper
735 beak form data set.

736 **Figure S14**. Two-dimensional morphospaces with phylogenetic tree mapped for the 15-taxon
737 lower beak form data set.

738 **Figure S15**. Major shape changes in cranium based on 8-taxon data set.

739 **Figure S16**. Major shape changes in upper beak based on 9-taxon data set

740 **Figure S17**. Major shape changes in lower beak based on 15-taxon data set

741 **Figure S18**. Two-dimensional functional morphospaces for the 8-taxon mandibular function data
742 set

743 **Figure S19**. Two-dimensional functional morphospaces for the 9-taxon mandibular function data
744 set

745 **Note S1**. Functional characters for disparity analysis

746 **Note S2**. Disparity analysis of functional characters.

747 **Note S3**. Principal coordinate (PCO) correlation with functional characters.

748 **Note S4**. Scaling the phylogenetic tree.

749 **Note S5**. Blomberg's K statistic and permutation test.

750 **Note S6**. Non-phylogenetic and phylogenetic comparative methods.

751 **Note S7**. Morphological variation of oviraptorosaur skull forms shown by 2D geometric
752 morphometrics.

753 **Note S8**. Correlation between overall mandibular form and its components shown by two-block
754 partial least square (2B-PLS) analysis.

755 **Note S9**. Implications of the differences in the integration level of the mandibles of caenagnathids
756 and oviraptorids.

757 **Note S10**. Results of disparity analysis of caenagnathids and oviraptorids.

758 **Note S11**. Discussion on disparity analysis of caenagnathids and oviraptorids.

759 **Note S12**. Results of disparity analysis of Ganzhou oviraptorids.

760 **Note S13**. Discussion on niche partitioning within Ganzhou oviraptorids.

761